# Evaluating the law of the wall in two-dimensional fully developed turbulent channel flows

E.-S. Zanoun and F. Durst[a)]
*Institute of Fluid Mechanics (LSTM), Friedrich-Alexander-Universität Erlangen-Nürnberg, Cauerstr. 4, D-91058 Erlangen, Germany*

H. Nagib
*Illinois Institute of Technology (IIT), Chicago, Illinois 60616*

(Received 17 December 2002; accepted 18 July 2003)

This article is concerned with the mean velocity distributions of two-dimensional fully developed turbulent plane-channel flows. To yield reliable information, the authors performed detailed hot-wire measurements for more than 12 Reynolds numbers. The experimental investigations covered a wide range of the Reynolds numbers up to $\mathrm{Re}_\tau \approx 5\times 10^3$, where $\mathrm{Re}_\tau$ is based on the wall friction velocity and the channel half-height. From the distribution of the mean velocity gradient $(dU^+/dy^+) = f(y^+)$ the entire flow field was analyzed, resulting in a logarithmic region for the mean velocity profile in the inertial sublayer, extending almost up to the center of the channel at higher Reynolds numbers. The analysis of the experimental results yield a value of the von Kármán constant, $\kappa$, close to $1/e(\approx 0.37)$ independent of the Reynolds number and the additive constant $B=3.70$, which is close to $10/e$, i.e., $U^+ = e \ln y^+ + 10/e = (1/0.37)\ln y^+ + 3.70$.  [DOI: 10.1063/1.1608010]

## I. INTRODUCTION AND AIM OF THE WORK

Research on turbulent flows basically started with the discovery of Reynolds in 1883 that pipe flows, depending on a dimensionless number later named the Reynolds number, consist of basically two different modes, either laminar or turbulent. Reynolds[1] also found that the transition from the laminar to the turbulent mode sets in intermittently by "flashes" that occur in localized regions when the Reynolds number exceeds a so-called. "critical" value. As the Reynolds number increases, the frequency of these "flashes" increases until a state of fully developed turbulence is obtained in the downstream direction of the so-called core region. All these fundamental properties of pipe flows were later found to represent common features of wall-bounded flows and, hence, also occur in nominally two-dimensional channel flows, the flow investigated by the present authors. The present investigations were carried out in air-driven plane-channel of aspect ratio (width/height) 12:1, covering a wide range of Reynolds number up to $\mathrm{Re}_\tau \approx 5\times 10^3$. The basic measuring technique employed in this work was hot-wire anemometry.

The authors' research into nominally two-dimensional fully developed turbulent plane-channel flow was triggered by recent publications containing suggestions for the normalized mean velocity distribution in the so-called overlapping region of the flow, being either a logarithmic or a power law (see, e.g., works by Barenblatt *et al.*,[2,3] Wosnik *et al.*,[4] and Österlund *et al.*,[5,6] and also the early work of von Kármán,[7] Prandtl,[8,9] Taylor,[10] and Millikan[11]). From that previous work, it was concluded that the turbulent velocity profiles in plane channel flows should obey a logarithmic law, $U^+ = (1/\kappa)\ln y^+ + B$. The arguments by Barenblatt *et al.*,[2,3] in particular, convinced the present authors to look again at the mean velocity profile of two-dimensional fully developed plane-channel flows. A further motivation for the current work also resulted from questions regarding the accuracy of the experimental data, especially at high enough Reynolds number flows. A wide scatter in values of the constants of the logarithmic law of the law was found in the literature. A summary of previous results found in the literature for both the von Kármán, $\kappa$, and the additive constants, $B$, is given in Figs. 1(a) and 1(b), respectively.

This scatter could be attributed either to inconsistencies in the general trends of the available experimental data which might be related to improper measuring equipment, the measurement of the wall friction velocity, $u_\tau$, or to low Reynolds number, i.e., $\mathrm{Re}_\tau \leq 10^3$, effects (see, e.g., Ref. 12). Furthermore, theoretical postulations of flow behavior can yield wrong $\kappa$-values. This encouraged the authors to extend the existing experimental data, applying more robust measuring and analysis techniques.

It was also a clear aim of the present work to carry out an analysis of the experimental data without any hypothesis about the structure of the turbulent wall-bounded channel flows. Hence the authors' experiments, aimed at direct measurements of the time-averaged velocities and from that the mean velocity gradient, $(dU^+/dy^+)$, was intended to give direct measurements of the small term in the corresponding momentum equation. From $\ln(dU^+/dy^+) = f(\ln y^+)$ the value of the von Kármán constant, $\kappa$, of the logarithmic law of the wall was derived. With this consistent approach, the

[a)]Author to whom correspondence should be addressed. Telephone: +49/9131/8529501; fax: +49/9131/8529503. Electronic mail: durst@lstm.uni-erlangen.de

 

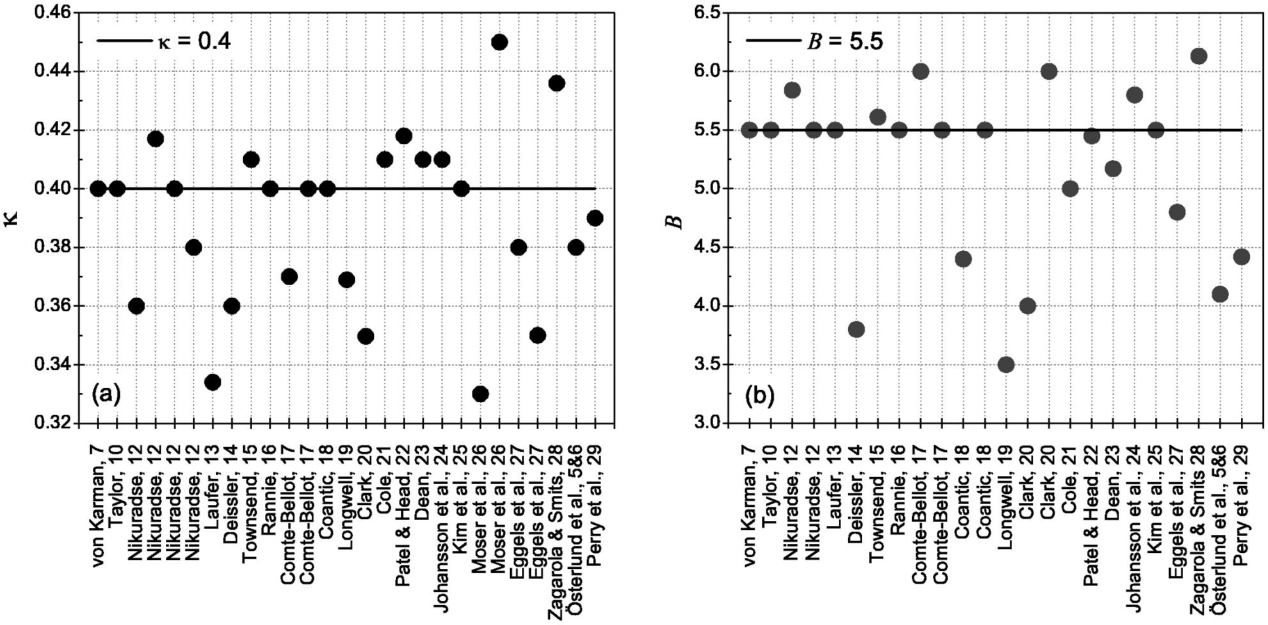


FIG. 1. Values of the constants of the logarithmic law of the wall obtained from various investigations: (a) von Kármán constant, $\kappa$ and (b) additive constant $B$.

authors aimed at obtaining reliable information regarding the mean velocity distribution in two-dimensional fully developed turbulent plane-channel flow. A wide range of the Reynolds number was covered and in this range an overall picture resulted regarding the $\mathrm{Re}_\tau$ dependence of the time-averaged velocity profile. For the high $\mathrm{Re}_\tau$ range of the flow, the analysis of the authors' experimental results indicates the existence of a "logarithmic mean velocity distribution," with a von Kármán constant, $\kappa$, close to $1/e(\approx 0.37)$. The experimental results and their analysis yielding this result are described in some detail. Other interesting features of the mean flow investigations are also reported.

## II. GOVERNING EQUATIONS AND CLASSICAL THEORIES

As far as the mean properties of turbulent flows are concerned, they are best described by the mean continuity and mean momentum equations, the so-called Reynolds equations. If these are adapted to the two-dimensional fully developed turbulent plane-channel flow, the following normalized equation results:

$$\frac{dU^+}{dy^+}=\left[1-\frac{y^+}{\mathrm{Re}_\tau}\right]+\overline{u_1'u_2'}^+, \tag{1}$$

where the normalization of all these terms in the equation is carried out with the following characteristic velocity, length and time scales:

$$u_c=u_\tau=\sqrt{\tau_\omega/\rho}, \quad l_c=\nu/u_\tau, \quad t_c=\nu/u_\tau^2. \tag{2}$$

Here $\mathrm{Re}_\tau$ is defined as $\mathrm{Re}_\tau=(u_\tau H/2)/\nu$, $H$ being full of the channel height.

Considerations suggested that the data to be measured to analyze flows described by Eq. (1) should be either $(dU^+/dy^+)$ or $-\overline{u_1'u_2'}^+$. If one of these quantities is known from experiments, the other can be deduced using the above mean momentum equation. In the region close to the wall, both of these terms vary strongly. If one is interested in the $U^+(y^+)$ distribution, one should measure $(dU^+/dy^+)$ directly and deduce from it the $U^+$-variation with $y^+$. To measure or to model $-\overline{u_1'u_2'}^+$ in the region where it is the much larger term in Eq. (1) is not the right way to get $U^+(y^+)$ deduced correctly. A small error in the $-\overline{u_1'u_2'}^+$ will yield a large error in the deduced $U^+(y^+)$ distribution.

To obtain a differential equation from Eq. (1) for the derivation of $U^+=F(y^+)$, early attempts with wall-bounded turbulent flows concentrated on the derivation of equation for the turbulent momentum transport term $-\overline{u_1'u_2'}^+$. Prandtl[8,9] developed an expression for the normalized momentum transport based on a mixing length hypothesis:

$$-\overline{u_1'u_2'}^+=l^{+2}\left|\frac{dU^+}{dy^+}\right|\frac{dU^+}{dy^+}. \tag{3}$$

He suggested that the mixing length increases linearly with the wall distance, i.e., $l^+=\kappa_P y^+$, where $\kappa_P$ is a constant.

On the basis of mainly dimensional considerations, von Kármán[7] proposed the following expression for the normalized turbulent transport term

$$-\overline{u_1'u_2'}^+=\kappa_K^2\left|\frac{(dU^+/dy^+)^3}{(d^2U^+/dy^{+2})^2}\right|\frac{dU^+}{dy^+}, \tag{4}$$

where $\kappa_K$ was suggested to be a constant and was found by various investigations to lie in the range $0.334\leqslant\kappa\leqslant 0.436$.

Just to give one further example, Deissler[13] proposed some kind of a damping function to take wall effects on the turbulent momentum transport term into account, yielding

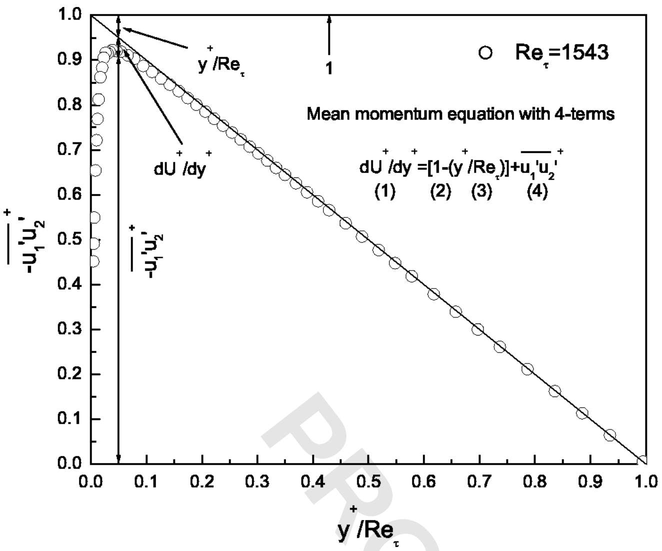


FIG. 2. Magnitude of the four terms in the mean momentum equation. Equation (1), for two-dimensional fully developed turbulent plane-channel flow.

$$-\overline{u_1'u_2'}^+ = c^2U^+y^+[1-\exp(-c^2U^+y^+)]\frac{dU^+}{dy^+}. \tag{5}$$

In this equation, $c$ was taken as a constant and was determined experimentally to be $c=0.124$. Some other attempts have been made to derive expressions for $-\overline{u_1'u_2'}^+$, e.g., those of Taylor[10] and Reichardt,[14] but their considerations do not bring further knowledge into the argument to be provided here. Hence no further references to the literature on $-\overline{u_1'u_2'}^+$ derivations are given at this point.

The above approaches to treat $-\overline{u_1'u_2'}^+$ "theoretically" and then to deduce from Eq. (1) a relationship for $U^+=F(y^+)$ have often been utilized in the literature but are far from being optimum to deduce $U^+$ information. This is readily seen from Fig. 2, which shows the four terms in Eq. (1) indicating that, over a large and the most important part of the flow, at least for this study, $(dU^+/dy^+)$ is the smallest term of the four. Hence this term is more sensitive to "modeling inaccuracies" occurring from the assumptions, e.g., introduced by Eqs. (3)–(5).

In general, it can be said that it is not a good approach to model the $-\overline{u_1'u_2'}^+$ term in Eq. (1) and then to deduce information about $U^+=F(y^+)$, i.e., the functional relationship for the normalized mean velocity profile. In spite of this general conclusion drawn from Fig. 2, the generally adapted analytical approaches are still the usual means for obtaining $U^+$ information, as proposed in the early work of von Kármán,[7] Prandtl,[8,9] Taylor,[10] Deissler,[13] etc. For the experimental work described in this article, the authors chose a different approach for the analysis of their data. Searching for a logarithmic velocity profile, the analysis of $\ln(dU^+/dy^+)=f(\ln y^+)$ has been done having the advantage that it does not contain an additive constant of the law of the wall in the case when a real logarithmic velocity profile exists.

## III. EXPERIMENTAL APPARATUS AND MEASURING TECHNIQUES

### A. Wind tunnel and channel test section

The experiments were carried out at LSTM, using the channel flow test section sketched in Fig. 3(a). The dimensions of the cross-section of the channel were 600×50 mm, providing a channel aspect ratio of 12:1. This aspect ratio was considered large enough, e.g., Dean,[15] recommended 7:1, to ensure the required two-dimensionality of the investigated turbulent, plane-channel flows. The total length of the channel setup was 6500 mm, corresponding to an $L/H$ ratio of 130. The flow was triggered at the channel entrance using well-organized tap letters such as X by using DYMO Label Printers. Seven rows of such stripes were used for tripping the flow, as can be seen from Fig. 3(b), and each row had a height of approximately 0.75 mm. The actual measuring location was taken at a distance from the channel inlet of $x=115\times H$. This length was considered to be sufficient to ensure a fully developed turbulent channel flow before reaching the measuring test section (see, e.g.,) Ref. 16, and was far enough away from the channel outlet to ensure no outlet

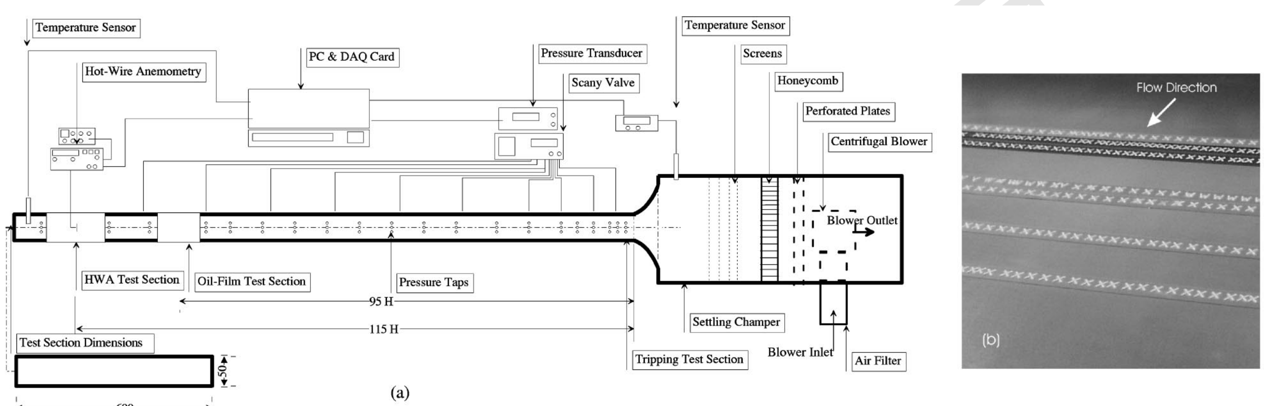


FIG. 3. (a) Sketch of the channel flow test setup with the temperature, pressure, shear stress and velocity measuring equipment and (b) photograph showing the tripping device (DYMO Brand X-letter).

disturbances to the flow. Hence prior to carrying out the actual measurements, the conditions were set up correctly to ensure by carefully choosing the channel dimensions and measuring locations, the two-dimensionality of the flow and its state of full development. The actual air flow was provided by a centrifugal blower. Its outlet was connected to a well-designed settling chamber to ensure the uniformity of the flow entering the channel inlet cross-section. After the outlet of the blower, in the downstream direction, the first essential flow control in the plenum chamber was located, consisting of two perforated plates with 52% of the cross-section consisting of $10\times10$ mm$^2$ openings and separated by 30 cm distance from the blower and each other. The second flow controlling part in the plenum chamber was a ''honeycomb plate'' with a mesh size of 8 mm diameter and a total length of the tubes of 160 mm. These passive flow control devices inside the plenum chamber were located in such a way as to yield a well-controlled inlet flow to the actual channel test section. The entire flow was setup in accordance with Loehrke and Nagib.[17]

The flow rates at the investigated $\mathrm{Re}_\tau$ were controlled by changing the speed of the radial blower blades by means of a frequency converter control unit, providing impeller rotational speeds of approximately 100–2000 rpm. This corresponded to a mean velocity range of the channel flow from 3 to 75 m/s with a centerline turbulence level of less than 0.3% at the axis of the channel inlet cross section. For all the measurements, the mean flow velocity through the channel entrance was measured using a Pitot tube. The outlet of the Pitot tube was connected to a precision pressure transducer operated by a computer with a 16-bit DAQ card. The mean flow velocity was used to compute the mean-based Reynolds number of the flow as

$$\mathrm{Re}_m=\frac{\overline{U}H/2}{\nu}. \tag{6}$$

Hence, as the above description shows, the test facility was designed carefully to carry out measurements over a wide range of Reynolds numbers up to $\mathrm{Re}_m\approx1.2\times10^5$.

## B. Measuring techniques

### 1. Pressure measurements

To provide the basis for the analysis of the authors' data, as reported in Sec. IV, pressure measurements were carried out to obtain the wall shear stress, $\tau_w$, for each investigated $\mathrm{Re}_m$ of the flow. For this purpose, pressure tappings were installed along the test section's top wall (the wide side of the cross section). These were employed over a 5 m length of the test section, where 19 pressure tappings were located to provide the streamwise pressure gradient, $\mathrm{d}P/\mathrm{d}x$, distribution for each investigated flow. Three static pressure tappings were installed at each of the 19 pressure-measuring locations, one at the centerline of the channel and two on both sides, 10 cm apart from the center point. Care was taken to ensure that the inner surface of the top side of the channel where the holes were drilled was free from drilling problems (i.e., smoothness was insured around the pressure tappings). All pressure measurement points were connected to a scanning valve to facilitate switching from one point to another and the corresponding static pressure was then measured and recorded for different air flow velocities (see Fig. 4). It is clear from Fig. 4 that the flow field was fully developed for all cases under investigation at least as far as the pressure distribution in the flow direction is concerned. In addition to the pressure measurements and corresponding to the air stream temperature in the channel, the air density and kinematic viscosity were calculated for the purpose of normalization using the following relations for density,

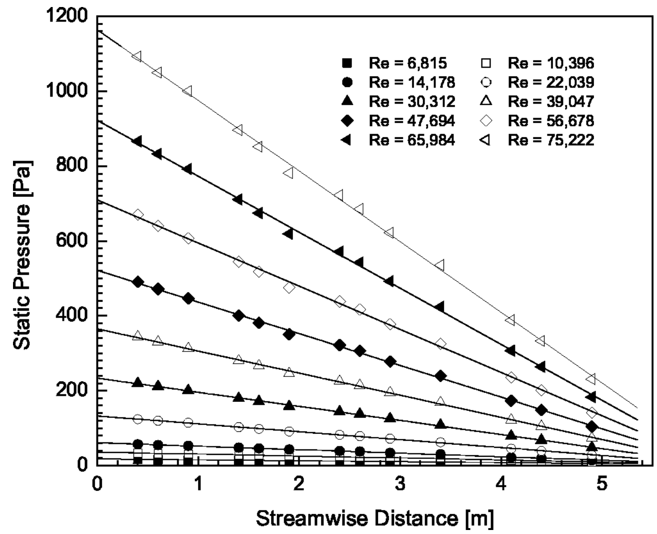

FIG. 4. Pressure gradient distributions along part of the channel at different Reynolds numbers.

$$\rho=\frac{(P_{\mathrm{atm}}+P_{\mathrm{st}})}{\Re T}, \tag{7}$$

and Sutherland's correlation for the kinematic viscosity,

$$\nu=1.458\times10^{-6}\frac{T^{3/2}}{\rho(T+110.4)}, \tag{8}$$

where $P_{\mathrm{atm}}$ is the atmospheric pressure and $\Re=279.1$ J/kg K is constant for air under the ideal gas law.

The mean static pressure, $P_{\mathrm{st}}$, measurements in Fig. 4 were used to evaluate the static pressure gradient, $\mathrm{d}P/\mathrm{d}x$, which in turn was employed to obtain the wall shear stress and the wall friction velocity, $u_\tau$, as follows:

$$\tau_w=-\frac{H}{2}\left(\frac{\mathrm{d}P}{\mathrm{d}x}\right),\quad u_\tau=\sqrt{\frac{\tau_w}{\rho}}. \tag{9}$$

As a result, the wall skin friction data were obtained independently of the velocity profile using the pressure gradient measurements provided in Fig. 4. Thereafter, the wall friction velocity, $u_\tau=\sqrt{\tau_w/\rho}$, and the kinematic viscosity, $\nu$, were used for scaling all results to yield the normalized velocity distribution over the channel half-width.

### 2. Oil film interferometry

Accurate and preferably independent/direct measurement of the wall-shear stress is of primary importance for determining the exact values of the constants of the law of

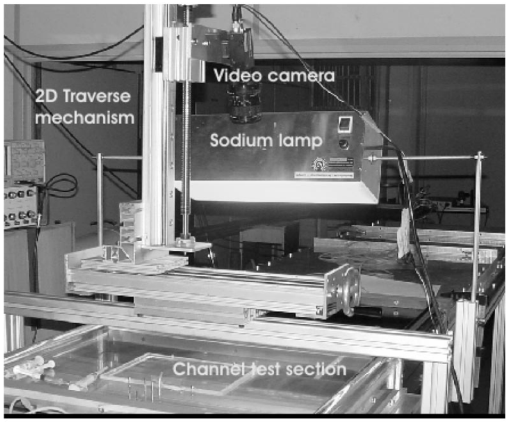


FIG. 5. Photograph of the oil-film optical test setup.

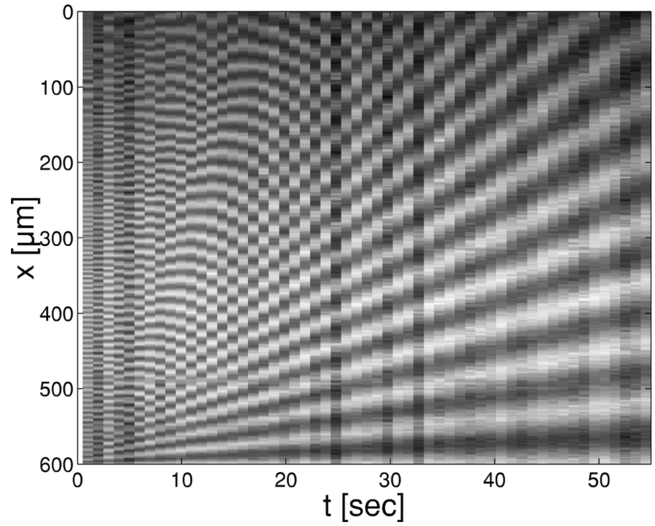


FIG. 6. Oil film thickness development over the $x-t$ diagram for a constant wall shear stress.

the wall. Oil film interferometry is a promising direct technique to obtain accurate values of the wall friction data. The basic concept of the oil film to measure the wall shear stress is to follow the movement of fringes which result from the interference pattern of a thin film illuminated by monochromatic light, see Tanner and Blows[18] and Fernholz *et al.*[19]

An oil film of thickness $h=h(x,t)$ is placed inside the test section where wall shear stress measurements are desired. Figure 5 shows a photograph of the oil film setup with the channel test section. The oil film is then driven by the imposed wall shear stress, $\tau(x,h,t)$, at the free surface, and therefore the stress can be evaluated experimentally by measuring $h(x,t)$. The variation of the oil film thickness in a two-dimensional flow is given by

$$\frac{\partial h}{\partial t}+\frac{\tau h}{\mu}\frac{\partial h}{\partial x}+\frac{h^2}{2\mu}\frac{\partial \tau}{\partial x}=0. \tag{10}$$

Equation (10) states that to obtain a value of the wall shear stress, it is necessary to measure $h$, $\partial h/\partial x$, and $\partial h/\partial t$. For fully developed flow, $\partial \tau/\partial x=0$, and therefore Eq. (10) reduces to

$$\frac{\partial h}{\partial t}+\frac{\tau h}{\mu}\frac{\partial h}{\partial x}=0. \tag{11}$$

Equation (11) shows that $h$ is constant in an $x-t$ plane along characteristic trajectories and the inverse slope of these trajectories, contour lines, is

$$u_k=\frac{\mathrm{d}x}{\mathrm{d}t}=\frac{\tau h}{\mu}, \tag{12}$$

expressing the rate of fringe movement, $u_k$, which is usually generated by cutting the captured images (see Fig. 6). Hence the fringe velocities, $u_k$, are obtained from an arbitrary number of fringes, $k$ (about 10). As a result, the skin friction information is obtained and the solution of Eq. (11) gives the wall shear stress:

$$\tau_w=\mu u_k\frac{2[n^2-\sin^2\alpha]^{1/2}}{\lambda[k+h_0/\Delta h]}, \tag{13}$$

where $h_0$ is the height of the zeroth black fringe at the film edge (i.e., $k=0$), $h_k$ is the height of the film at the $k$th black fringe, and $\Delta h$ is the height difference between two consecutive fringes:

$$\Delta h=\frac{\lambda}{2[n^2-\sin^2\alpha]^{1/2}}, \tag{14}$$

where $\lambda$ is the light wavelength, $n$ is the refractive index of the oil, and $\alpha$ is the camera viewing angle. Values of $\mu$, $n$, $\alpha$, and $\lambda$ are usually given and from the $x-t$ diagram an arbitrary number of fringe velocities, $u_k$, are measured. The authors have carried out an error analysis using Eq. (13) to evaluate the accuracy of the oil film technique finding that it lies within $\pm 2.5\%$. The major uncertainty for this accuracy arises from the accuracy of the oil viscosity measurements.

### *3. Hot-wire anemometry*

The velocity profile measurements reported in this article were carried out using a DANTEC 55M10 constant-temperature anemometer. To adjust the system, the instructions provided in the manual were followed, both for the calibration of the system and for its employment for the present channel flow investigations. The hot-wire measurements of the local velocity were carried out with a boundary layer probe (DANTEC, Type 55P15), equipped with a wire of 5 $\mu$m diameter and an active wire length of 1.25 mm, providing an aspect ratio, $l/d$, of 250. Hence the wire had a sufficiently large aspect ratio to suggest a negligible influence of the prongs on the actual velocity measurement. All calibrations and measurements were performed with an 80% overheat ratio, $a=(R_w-R_a)/R_a$, where $R_w$ is the operational hot-wire resistance and $R_a$ is the resistance of the cold wire, i.e., at ambient air temperature. Before each set of measurements, the hot-wire probe was calibrated against velocity measured with a Pitot tube at the channel entrance where a uniform and well-defined flow field existed. The Pitot tube was installed directly at the centerline of the channel input cross-section and its output was connected to a precision pressure transducer for both stagnation, $P_0$, and static, $P_{st}$, pressure measurements. The pressure transducer, Valdyne differential type, was used for measuring the pressure with an accuracy of $\pm 0.25\%$. In addition, the air temperature inside the tunnel was measured at all times during measurements within accuracy range of $\pm 0.05\,^{\circ}\mathrm{C}$. To obtain the velocity dynamic head of the Pitot tube, the mean static pressure was measured 25 mm downstream of the Pitot probe.

Along a streamline at the input of the channel centerline, integrating the momentum equation results in the well-known Bernoulli equation, which applies between a point in the flow and stagnation point on the same streamline:

$$\frac{P_0}{\rho}=\frac{P_{st}}{\rho}+\frac{\overline{U}^2}{2}, \tag{15}$$

where $\rho$ is the air density. By rearranging the terms of the above equation, the mean velocity, $\overline{U}$, of the air flow at channel entrance was obtained, $\overline{U}=[2(P_0-P_{st})/\rho]^{1/2}$.

Hence, the time-averaged air velocity for calibration was simply calculated by measuring the pressure difference between the stagnation pressure, $P_0$, and the static pressure, $P_{st}$, using a differential pressure transducer. The ambient conditions were monitored before and during each test run using an electronic barometer and thermometer. All measuring equipment were connected to an A/D converter board from National Instruments with 16 bit resolution and 8 input channels. In addition, a computer-based programming system was used for acquiring and processing all the measured data.

To employ the calibration data for the hot-wire measurements, a fourth-degree polynomial fit was chosen for fitting the calibration data with an accuracy of better than $\pm 1\%$. To ensure that the original calibration curve was maintained during one entire set of hot-wire measurements, the calibration curves were rechecked after each set of measurements covering the entire range of velocities experienced in the wall region for each investigated flow case. If the deviations of the calibration were more than $\pm 1\%$, the entire set of data was rejected and the measurements for the corresponding $\mathrm{Re}_\tau$ were repeated.

#### *4. Wall distance*

Great care was taken to ensure a precise location of the hot wire at a reference distance from the wall. A calibration positioning procedure proposed by Bhatia *et al.*[20] and Durst *et al.*[21] was applied; it is given with more detail in Durst *et al.*[22] The location of the hot wire, therefore, in the vertical direction was adjusted by measuring the HWA output at zero flow velocity in the channel as close as possible to the channel wall surface, and from the position calibration line the corresponding position of the wire was estimated. The absolute error in the wire positioning was $\pm 5\ \mu$m.

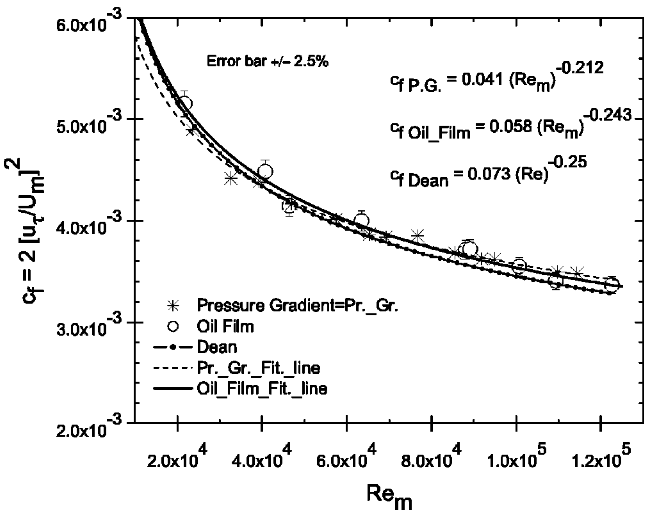


FIG. 7. Measured skin friction coefficient from the pressure gradient and the oil film interferometry compared with Ref. 15.

## IV. RESULTS AND ANALYSIS

Employing the measuring techniques described in Sec. III B, the authors carried out experiments for the following Reynolds numbers, based on the wall friction velocity and the channel half-height:

$$\mathrm{Re}_\tau = 1167,1543,1850,2155,2573,2888,$$
$$3046,3386,3698,3903,4040,4605,4783.$$

In wall-bounded turbulent flows, the wall shear stress is conventionally expressed in terms of the local skin friction coefficient, i.e., in dimensionless form, as

$$c_f=\frac{\tau_w}{\frac{1}{2}\rho\overline{U}^2}. \tag{16}$$

By introducing the wall friction velocity, $u_\tau=\sqrt{\tau_w/\rho}$, Eq. (16) can be rearranged to yield

$$c_f=2\left[\frac{u_\tau}{\overline{U}}\right]^2. \tag{17}$$

Therefore, by means of Eq. (17), it was easy to determine the wall skin friction coefficient experimentally by measuring the integral flow parameters, $\overline{U}$, $T$, and $\mathrm{d}P/\mathrm{d}x$, or the rate of fringe movement of the oil film, $u_k$. The resultant data for the wall skin friction coefficient which were obtained from both the pressure gradient and the local measurements by oil film are presented in Fig. 7. Good agreement of the wall skin friction data was found between the pressure gradient and the oil film, which supports the two-dimensionality of a channel of 12:1 aspect ratio. The data in Fig. 7 also compared well with Dean's[15] formula:

$$c_f = 0.073\,\mathrm{Re}^{-0.25}, \tag{18}$$

where Re is based on the channel full-height and, from the error analysis, the shear stress measurements were found to be accurate within $\pm 2.5\%$ of the mean values. As a result,

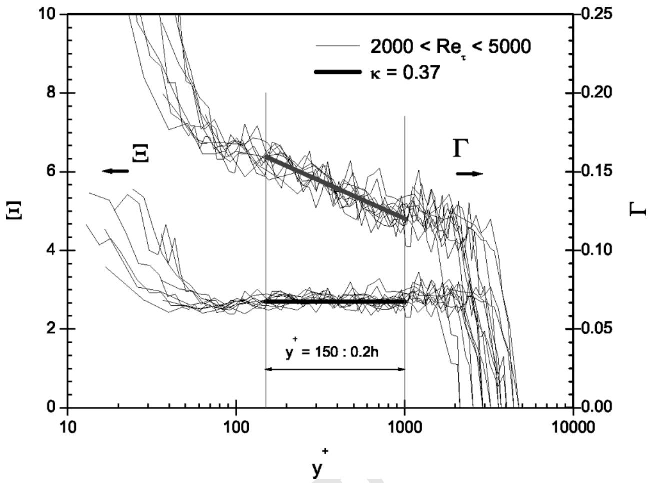


FIG. 8. Diagnostic functions for the law of the wall.

the present work suggests the following modified equation for representation of the wall skin friction data:

$$c_f = 0.058\,\mathrm{Re}_m^{-0.243}. \tag{19}$$

Utilizing the wall friction data, the present mean velocity distributions were normalized using the corresponding wall shear velocity, $u_\tau$, to yield the dimensionless mean velocity distribution, $U^+ = F(y^+)$. The resultant velocity profiles were then analyzed with respect to the question of whether the profile in the inertial sublayer behaves in a logarithmic manner, as proposed by Prandtl,[8,9] von Kármán,[7] and Millikan:[11]

$$U^+ = \frac{1}{\kappa}\ln y^+ + B, \tag{20}$$

where $\kappa$ is the von Kármán constant and $B$ is an additive constant.

The present study also embraced the question of whether the velocity profile obeys a power law as proposed in the earlier investigations of Millikan,[11] and more recently suggested by Barenblatt *et al.*[2,3] and Wosnik *et al.*,[4] i.e., in the form

$$U^+ = C y^{+\gamma}. \tag{21}$$

where $C$ and $\gamma$ are empirical constants, but are often Reynolds number dependent.

Further, to see more clearly the effect of the Reynolds number on the mean velocity profile, the following diagnostic functions recently suggested by Österlund *et al.*[5,6] and Wosnik *et al.*[4] are introduced:

$$\Xi = y^+ \frac{dU^+}{dy^+}, \quad \Gamma = \frac{y^+}{U^+}\left[\frac{dU^+}{dy^+}\right], \tag{22}$$

which represent the normalized slopes of the mean velocity distribution in either the logarithmic or the power region, respectively, and the behavior of both functions is shown in Fig. 8.

A constant behavior of $\Xi$ for high enough Reynolds numbers leads to the existence of a logarithmic layer supporting Millikan's,[11] argument that a logarithmic law is expected in a high Reynolds number turbulent channel flow with a constant value of the von Kármán constant. In the inertial sublayer, all $\Xi$ profiles in Fig. 8 showed a constant slope at $y^+ \geqslant 150$, which means that the logarithmic law is a good representation of the mean velocity measured in the overlap region for $\mathrm{Re}_\tau \geqslant 2\times 10^3$ (see Ref. 38). In addition, a constant behavior of the power-law diagnostic function, $\Gamma$, indicates that the mean velocity profile should behave in a power form. However, the general trend of the power-law diagnostic function is a monotonic decrease when plotted versus wall distance, as shown in Fig. 8. Therefore, the power law is far from useful to describe the mean velocity profile in the overlap region (see, e.g., the work by Clauser,[24] who came to the conclusion that no universal values can be assigned to $C$ and $\gamma$). As a result, the behavior of the $\Xi$ function indicates clearly that the normalized mean velocity profiles of two-dimensional fully developed turbulent plane-channel flows is well described by a logarithmic velocity distribution.

To proceed further to obtain the exact value of the von Kármán constant of the logarithmic law of the wall, the authors adopted a new approach rather than following that in the earlier investigations (see, e.g., Refs. 5 and 6). The new approach mainly depends, as proposed by the authors, in both Secs. I and II, on the natural logarithm of the mean velocity gradient and for this purpose a selected sample of the data is shown in Fig. 9. The upper limit of each individual case where the logarithmic law can fit the data well was found to be higher than the traditional upper limit, i.e., $y^+ = 0.15(H^+/2)$ or $0.2(H^+/2)$, and it increases with increasing Reynolds number (see Fig. 9). This resulted in Fig. 10, indicating that the interval over which the logarithmic law could be applied increases with increasing Reynolds number and extends almost up to the center of the channel for the highest Reynolds number case (see, e.g., Refs. 25 and 26). However, the lower limit was found to be common and equal to $y^+ = 150$ for almost all the cases and the upper limit extends to $y^+ \approx 75\%$ of $(H^+/2)$, corresponding to the highest value of the Reynolds number. The results shown in Fig. 9 showed the same pattern where the logarithmic law fits the data well within the experimental error for different Reynolds numbers. Therefore, for the purpose of the current analysis, all the data shown in Fig. 8 were replotted in the range $50 \leqslant y^+ \leqslant 75\%$ of $(H^+/2)$ and are shown in Fig. 11; however, the fitting process only considered data from $y^+ = 150$ to avoid the overshoot of $U^+$ for small Re values. All the higher Reynolds numbers, i.e., $\mathrm{Re}_\tau > 1.5\times 10^3$, results corresponding to the different Reynolds numbers mentioned earlier showed the same pattern where the logarithmic law represents the data within the experimental error. The region where there was a good fit of the data to the logarithmic law was considered for the least-squares curve fit yielding a reliable value of the von Kármán constant. From Eq. (20) the logarithmic law of the wall can be rewritten as follows:

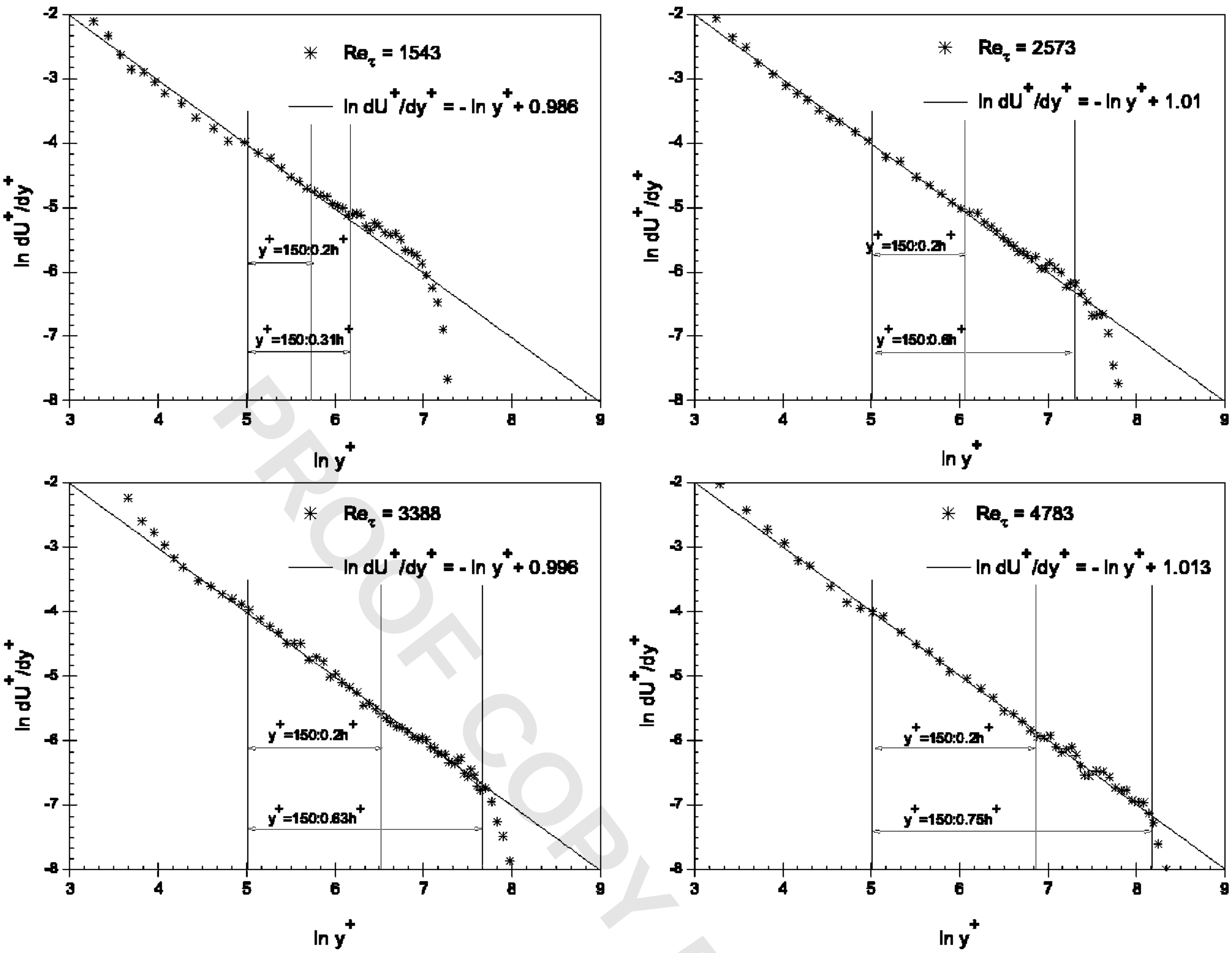


FIG. 9. Samples of mean velocity gradient for different Reynolds numbers, plotted double-logarithmically.

$$U^+ = \frac{1}{\kappa}\ln y^+ + B \Rightarrow \frac{dU^+}{dy^+} = \frac{1}{\kappa y^+} \Rightarrow \ln\left[\frac{dU^+}{dy^+}\right] = -\ln y^+ + \ln\left[\frac{1}{\kappa}\right]. \tag{23}$$

As a consequence, using an optimized least-squares curve fit for the best fit of every individual case over the new upper and lower limits resulted in a value of $1 \pm 2.5\%$ for the intercept ln $[1/\kappa]$ (see Fig. 9). As a result, the data in Fig. 11

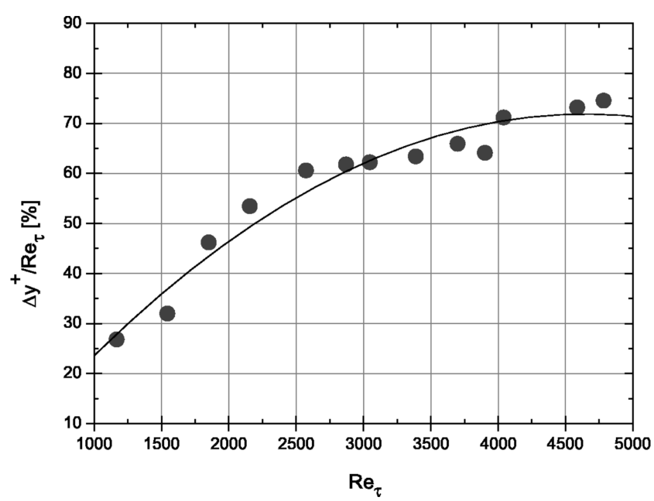


FIG. 10. Maximum extent of logarithmic law region represented using inner scale.

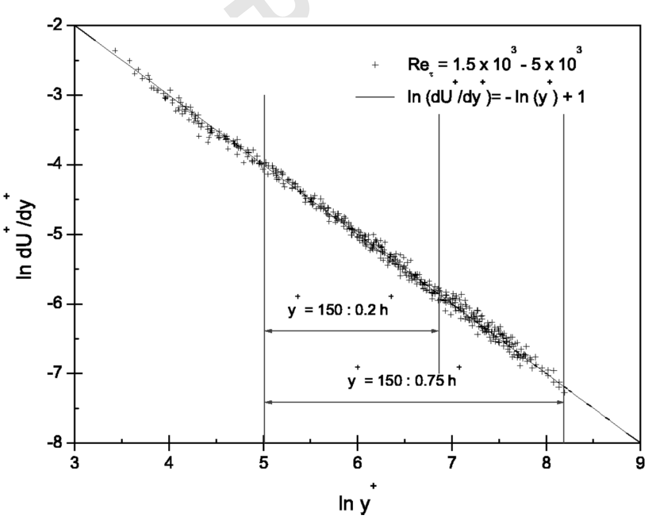


FIG. 11. A $\ln dU^+/dy^+ - \ln y^+$ representation of the mean velocity gradient over a wide.

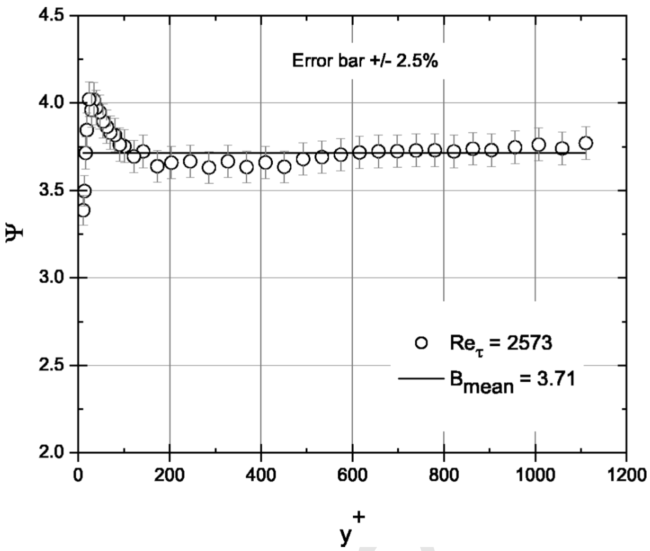


FIG. 12. The additive constant of the logarithmic law of the wall as a function of $y^+$.

suggest that there exists a functional relationship for the far distant region of the normalized mean velocity distribution and it is given by

$$\ln\left[\frac{dU^+}{dy^+}\right]=-\ln y^+ +1\pm 2.5\%. \tag{24}$$

Hence, taking the intercept in Eq. (24) equal to 1.0 (within an accuracy of measurements of $\pm 2.5\%$) results in

$$\ln\left[\frac{dU^+}{dy^+}\right]=-\ln y^+ +1 \Rightarrow \ln\left[y^+\frac{dU^+}{dy^+}\right]=1 \Rightarrow \left[y^+\frac{dU^+}{dy^+}\right]=e, \tag{25}$$

$$\kappa=\left[y^+\frac{dU^+}{dy^+}\right]^{-1}=\frac{1}{e}, \tag{26}$$

which is an interesting result deduced from the authors' experimental data. This readily suggests a logarithmic region for the far field of the normalized mean velocity profile with a von Kármán constant of $\kappa=1/e$.

The mean value of the second constant of the logarithmic law of the wall, an additive constant $B$, was obtained from the mean velocity profile as described below:

$$\Psi=U^+-\frac{1}{\kappa}\ln y^+. \tag{27}$$

A constant behavior of $\Psi$ (see Fig. 12) in the region where the logarithmic law is valid was considered for an average calculation over all Reynolds numbers.

The results are summarized in Fig. 13 for all the cases where the limits are $y^+=150$ and $y/(H/2)=0.20$ in comparison with the results over the author's new limits. From this figure, for $\mathrm{Re}_\tau \geqslant 2\times 10^3$, we found that following the traditional technique for data processing proposed by Österlund *et al.*[5,6] resulted in a von Kármán constant of 0.37, which is

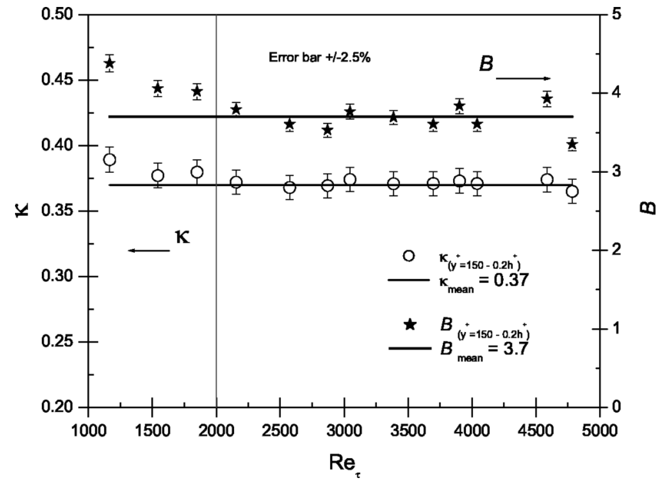


FIG. 13. Summary of the von Kármán constant and the additive constant versus $Re_\tau$.

very close to $\kappa=1/e$, obtained with the authors' new limits, and the mean value of the additive constant was found to be $B=3.7$, which is close to $10/e$.

## V. CONCLUSIONS, FINAL REMARKS, AND OUTLOOK

The present work concentrated on the normalized mean velocity distribution for two-dimensional fully developed turbulent plane-channel flows. A logarithmic velocity distribution was found, giving a good approximation of the velocity profile in a fairly large part of the channel core region, almost up to the center of the channel for high Reynolds number. However, the constants in the logarithmic profiles were found to vary with Reynolds number values of $\mathrm{Re}_\tau \leqslant 2\times 10^3$. For the high Reynolds number cases, i.e., for $\mathrm{Re}_\tau \geqslant 2\times 10^3$, limited values of the constants in the logarithmic velocity profile were found. The present data yield a value of the von Kármán constant, $\kappa$, close to $1/e(\approx 0.37)$ independent of the Reynolds number. Such a value was also claimed by Goldstik and Stern.[27] In addition, the additive constant in the authors' experiments was found to be $B=3.7$, which is close to $10/e$.

It is worth noting here that the logarithmic law was analytically deduced by Millikan,[11] using fundamental relationships obtained by Prandtl[8,9] and von Kármán.[7] Later, work by Yajnik[28] proposed a theory to describe pipe and channel flows using matched asymptotic expansions together with asymptotic hypotheses describing the order of various terms in the equations of mean motion and turbulent kinetic energy. Yajnik's theory leads to asymptotic laws corresponding to the law of the wall (the logarithmic law), the velocity defect law, and the law of the wake (see also work by Afzal and Yajnik,[29] Afzal,[30] Tennekes,[31] and Gill[32]).

More recently, based on the Liegroup symmetry method, Oberlack[33] has provided the first derivation of the log-law from that can be considered as first principles. It is obtained from the symmetry properties of the transport equation for the two-point, velocity-velocity, correlation function in the range of separations and distances from the wall that are large enough for viscous influence to be negligible.

The authors would like to stress that the above given values for $\kappa=1/e(\approx 0.37)$ and $B=3.7(\approx 10/e)$ result from careful measurements in a plane-channel flow for high Reynolds numbers. However, for low Reynolds number, i.e., $\mathrm{Re}_\tau<2\times 10^3$, both the von Kármán and the additive constants were found to be Reynolds number-dependent, (see, e.g., Ref. 34). It is worth mentioning that following the traditional technique for data processing proposed by Österlund *et al.*,[5,6] which applied to the overlap region where the logarithmic law fits the data well, resulted in a Reynolds number independence of the von Kármán constant for $\mathrm{Re}_\tau\geqslant 2\times 10^3$. If only data for $\mathrm{Re}_\tau\geqslant 2\times 10^3$ is used, $\kappa$ is found to be 0.37, which is in very close agreement with the present finding. It is also worth noting that the von Kármán constant, $\kappa$, obtained in this work significantly differs from the value deduced by Zagarola and Smits,[35] who found $\kappa=0.436$. This high value in the turbulent pipe flow suggests to apply hot wire and laser Doppler measurements in pipe flows and to apply the data analysis employed by the authors in this article.[36–49]

## ACKNOWLEDGMENTS

Funds received from LSTM-Erlangen to carry out the work and from the Universitätbund Erlangen-Nürnberg e.V. to build the test section are appreciated.

[1] O. Reynolds, ''On the dynamical theory of incompressible viscous fluids and determination of the criterion,'' Philos. Trans. **186**, 123 (1883).
[2] G. I. Barenblatt, ''Scaling laws for fully developed shear flows. Part 1. Basic hypotheses and analysis,'' J. Fluid Mech. **248**, 513 (1993).
[3] G. I. Barenblatt and A. J. Chorin, ''Scaling laws for fully developed shear flows. Part 2. Processing of experimental data,'' J. Fluid Mech. **248**, 521 (1993).
[4] M. Wosnik, L. Castillo, and W. George, ''A theory for turbulent pipe and channel flows,'' J. Fluid Mech. **421**, 115 (2000).
[5] J. M. Österlund, A. V. Johansson, H. M. Nagib, and M. H. Hites, ''Wall shear stress measurements in high Reynolds number boundary layers from two facilities,'' 30th AIAA Paper 99-3814, Fluid Dynamics Conference, Norfolk, VA (1999).
[6] J. M. Österlund, A. V. Johansson, H. M. Nagib, and M. H. Hites, ''A note on the overlap region in turbulent boundary layers,'' Phys. Fluids **12**, 1 (2000).
[7] T. von Kármán, ''Mechanische Ähnlichkeit und Turbulenz,'' Nachr. Ges. Wiss. Göettingen, Math.-Phys. Kl. ■■, 58 (1930).
[8] L. Prandtl, ''Uber die ausgebildete Turbulenz,'' Z. Angew. Math. Mech. **5**, 136 (1925).
[9] L. Prandtl, ''Zur turbulenten Strömung in Rohren und laengs Platten,'' Ergeb. Aerodyn. Versuch, Göttingen IV, Lieferung ■■, 18 (1932).
[10] G. I. Taylor, ''The transport of vorticity and heat through fluid in turbulent motion,'' Proc. R. Soc. London **135**, 685 (1932).
[11] C. M. Millikan, ''A critical discussion of turbulent flows in channels and circular tubes,'' in Proc. 5th Intl Congress of Appl. Mech. (1938), p. 386.
[12] M. Fischer, ''Turbulente wandgebundene Strömungen bei kleinen Reynoldszahlen,'' Dissertation, Universität Erlangen Nürnberg, 1999.
[13] R. G. Deissler, ''Analysis of turbulent heat transfer, mass transfer and friction in smooth tubes at high Prandtl and Schmidt numbers,'' NACA Tech. Rep. 12100 (supersedes NACA Tech. Note 3145, 1954) (1955).
[14] H. Reichardt, ''Vollständige Darstellung der turbulenten Geschwindigkeitsverteilungen in glatten Leitungen,'' Z. Angew. Math. Mech. **31**, 208 (1951).
[15] R. B. Dean, ''Reynolds number dependence of skin friction and other bulk flow variables in two-dimensional rectangular duct flow,'' ASME J. Fluid Eng. **100**, 215 (1978).
[16] G. Comte-Bellot, ''Turbulent flow between two parallel walls,'' Ph.D. thesis (in French) University of Grenoble (in English as ARC 31609), FM 4102 (1963).
[17] K. I. Loehrke and H. M. Nagib, ''Experiments on management of free-stream turbulence,'' AGARD Report No. 598, IIT, Chicago, IL (1972).
[18] L. H. Tanner and L. G. Blows, ''A study of the motion of oil films on surface in air flow, with application to the measurements of skin friction,'' J. Phys. E **2**, 194 (1976).
[19] H. H. Fernholz, G. Janke, M. Schober, P. M. Wagner, and D. Warnack, ''New developments and applications of skin-friction measuring technique,'' Meas. Sci. Technol. **77**, 1396 (1996).
[20] J. C. Bhatia, F. Durst, and J. Jovanović, ''Corrections of hot-wire measurements near walls,'' J. Fluid Mech. **122**, 411 (1982).
[21] F. Durst, R. Müller, and J. Jovanović, ''Determination of the measuring position in laser-Doppler anemometry,'' Exp. Fluids **6**, 105 (1988).
[22] F. Durst, E. S. Zanoun, and M. Pashtrapanska, ''In situ calibration of hot wires close to highly heat-conducting walls,'' Exp. Fluids **31**, 103 (2001).
[23] E. S. Zanoun, H. Nagib, F. Durst, and P. Monkewitz, ''Higher Reynolds number channel data and their comparison to recent asymptotic theory,'' 40th AIAA-1102, Aerospace Sciences Meeting, Reno (2002).
[24] F. H. Clauser, ''The turbulent boundary layer,'' Adv. Appl. Mech. **4**, 1 (1956).
[25] T. Wei and W. W. Willmarth, ''Reynolds number effects on the structures of a turbulent channel flow,'' J. Fluid Mech. **204**, 57 (1989).
[26] M. Gad-el-Hak and P. R. Bandyopadhyay, ''Reynolds number effect on wall-bounded flows,'' Appl. Mech. Rev. **47**, 307 (1993).
[27] M. A. Goldstik and V. N. Stern, ''Hydrodynamic laws and turbulence,'' Academy of Science of the Soviet Union, Siberian Dep., Institute for Thermal Physics, Novosibirsk (1977), p. 326 (in Russian).
[28] K. S. Yajnik, ''Asymptotic theory of turbulent shear flows,'' J. Fluid Mech. **42**, 411 (1970).
[29] N. Afzal and K. S. Yajnik, ''Analysis of turbulent pipe and channel flows at moderately large Reynolds number,'' J. Fluid Mech. **61**, 23 (1973).
[30] N. Afzal, ''Millikan's argument at moderately large Reynolds number,'' Phys. Fluids **19**, 600 (1976).
[31] H. Tennekes, ''Outline of a second-order theory of turbulent pipe flow,'' AIAA J. **6**, 1735 (1968).
[32] A. E. Gill, ''The Reynolds number similarity argument,'' J. Math. Phys. **47**, 437 (1968).
[33] M. Oberlack, ''A unified approach for symmetries in plane parallel turbulent shear flows,'' J. Fluid Mech. **427**, 299 (2001).
[34] G. D. Huffman and P. Bradshaw, ''A note on von Kármán constant in low Reynolds number turbulent flows,'' J. Fluid Mech. **53**, 45 (1972).
[35] M. V. Zagarola and A. J. Smits, ''Mean-flow scaling of turbulent flow,'' J. Fluid Mech. **373**, 33 (1998).
[36] J. Nikuradse, ''Gesetzmässigkeit der turbulenten Strömung in glatten Rohren,'' Forschg. Arb. Ing.-Wes. **356**, ■■ (1932).
[37] J. Laufer, ''Investigation of turbulent flow in a two-dimensional channel,'' Report 1053-National Advisory Committee for Aeronautics (1954), p. 1247.
[38] A. A. Twonsend, *The Structure of Turbulent Shear Flow* (Cambridge U. P., Cambridge, 1956).
[39] W. D. Rannie, ''Heat transfer in turbulent shear flow,'' J. Aeronaut. Sci. **23**(5), 485 (1956).
[40] M. Coantic, ''Contribution á l'étude de la structure de la turbulence dans une conduite de section cirulaire,'' Thèse doctorat d'état es sciences physiques, Univ. d'Aix-Marseille, 1966.
[41] P. A. Longwell, *Mechanics of Fluid Flow* (McGraw-Hill, New York, 1966).
[42] J. A. Clark, ''A study of incompressible turbulent boundary layers in channel flow,'' ASME J. Basic Eng. **90**, 455 (1968).
[43] D. Cole, ''The turbulent boundary layer in a compressible flow,'' The Rand Corporation, Re. R-403-PR (1968).
[44] V. C. Patel and M. R. Head, ''Some observations on skin friction and velocity profiles in fully developed pipe and channel flows,'' J. Fluid Mech. **38**, 181 (1969).
[45] A. V. Johansson and P. H. Alfredsson, ''On the structure of turbulent channel flow,'' J. Fluid Mech. **122**, 295 (1982).
[46] J. Kim, P. Moin, and R. Moser, ''Turbulence statistics in fully developed channel flow at low Reynolds number,'' J. Fluid Mech. **177**, 133 (1987).
[47] R. T. Moser, J. Kim, and N. N. Mansour, ''Direct numerical simulation of turbulent channel flow up to $Re_\tau=590$,'' Phys. Fluids **11**, 943 (1999).
[48] J. G. M. Eggels, F. Unger, M. H. Weiss, J. Westerweel, R. J. Adrian, R.

Friedrich, and F. T. M. Nieuwstadt, ''Fully developed turbulent pipe flow: A comparison between direct numerical simulation and experiment,'' J. Fluid Mech. **268**, 175 (1994).

[49] A. E. Perry, S. Hafez, and M. S. Chong, ''A possible reinterpretation of the Princeton superpipe data,'' J. Fluid Mech. **49**, 395 (2001).

[50] For the authors' own investigations of the side wall effect on the two-dimensionality of the flow at the channel centerline, new results are published in ''Measuring probe size, side wall and tripping effects on mean flow properties of turbulent channel flows,'' submitted to Journal of Fluids Engineering.